Electronic Supplementary Material (ESI) for Soft Matter

Supporting Information

Electrostatic *vs* covalent bond in modified Jeffamine: effect on the phase behaviour and on the templating of mesoporous silica

Nadia Canilho, Andreea Pasc*, Mélanie Emo, Marie-José Stébé and Jean-Luc Blin

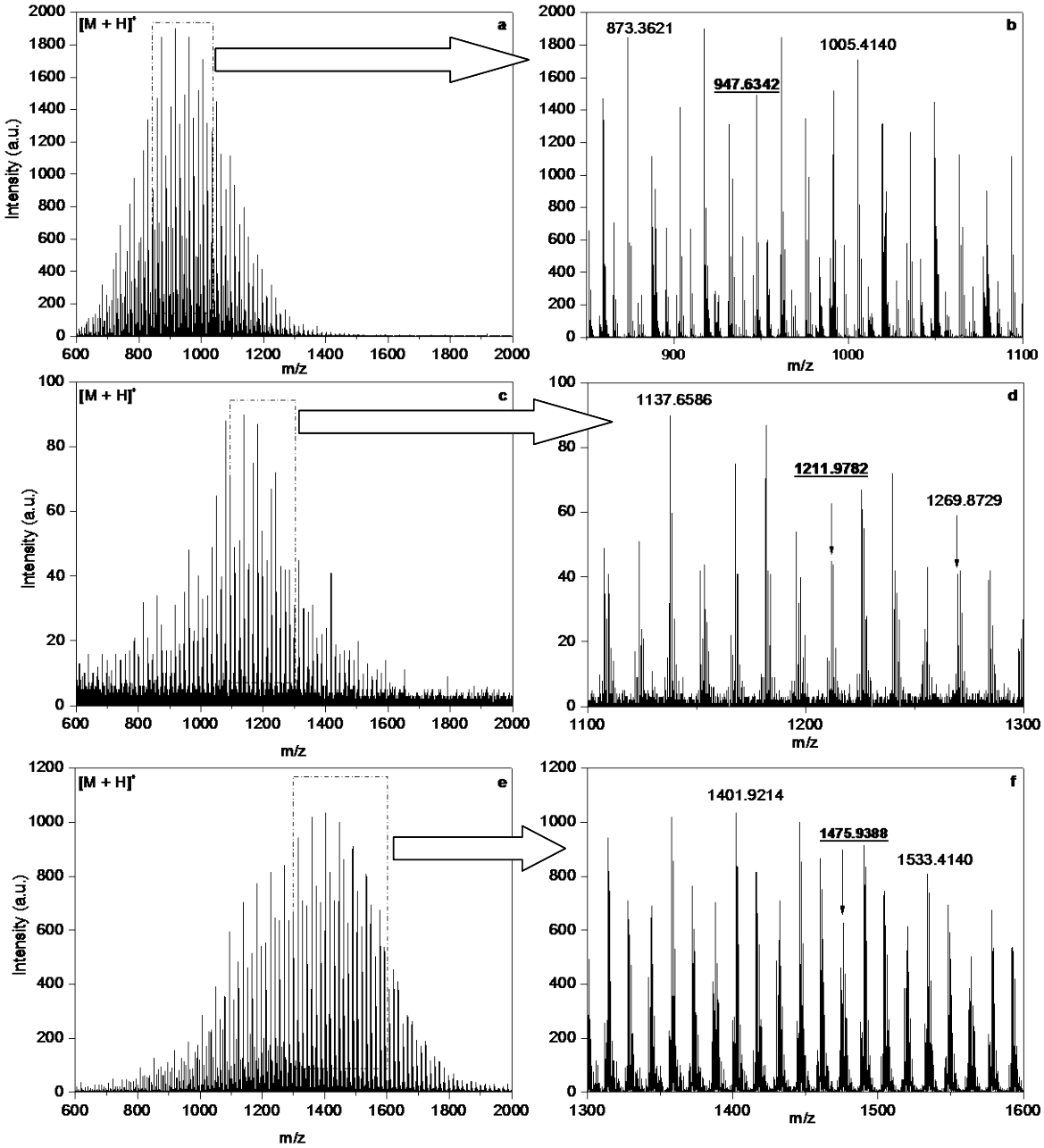

Figure S1. MALDI TOF spectra of (a,b) ED900, (c,d) mono-oleoyl Jeffamine and (e,f) di-oleoyl Jeffamine.

Table S1. X-Ray diffraction data for 54.6 wt% of $\mathbf{OOJ_{cat}}$ in water at 10°C indexed to the space group *Im3m* with a lattice parameter a = 7.4 nm

hkl	$(h^2+k^2+l^2)^{1/2}$	d_{obs} (nm)	d_{cal} (nm)	I_{obs}*
110	√2	5.2	5.2	vvs
200	√4	3.7	3.7	s
211	√6	3.0	3.0	s

* I_{obs} *are the observed intensities, which are ranged from vvs (extremely strong) to s (strong).*

Table S2. X-Ray diffraction data for 43 wt% of $\mathbf{OOJ_{cov\text{-}cat}}$ in water at 10°C indexed to the space group *Im3m* with a lattice parameter a = 8.4 nm

hkl	$(h^2+k^2+l^2)^{1/2}$	d_{obs} (nm)	d_{cal} (nm)	I_{obs}*
110	√2	5.9	5.9	vvs
200	√4	4.2	4.2	m
211	√6	3.4	3.4	s

* I_{obs} *are the observed intensities, which are ranged from vvs (extremely strong), s (strong) to m (medium).*

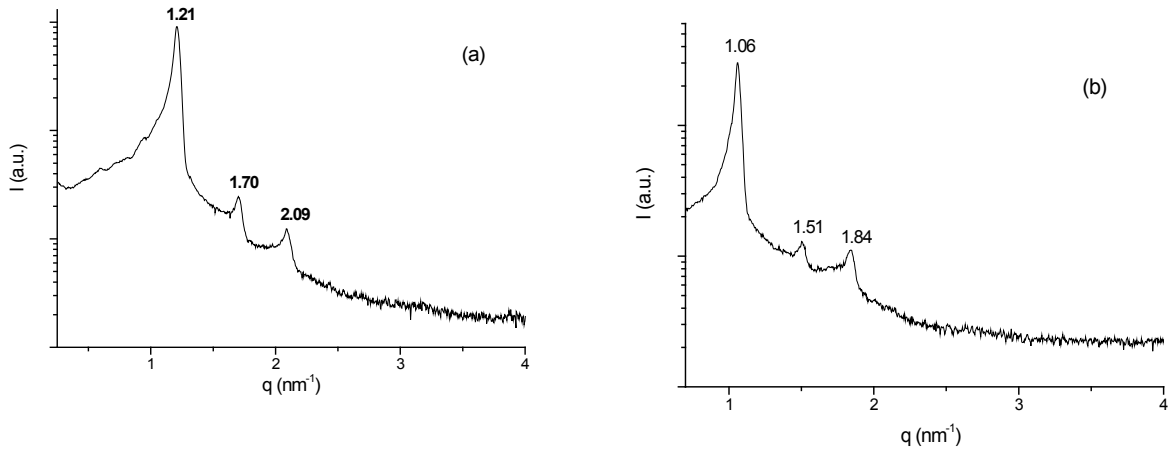

Figure S2. SAXS diffraction patterns obtained for (a) 54.6wt% of $\mathbf{OOJ_{cat}}$ and (b) 43 wt% of $\mathbf{OOJ_{cov\text{-}cat}}$ in water at 10°C.

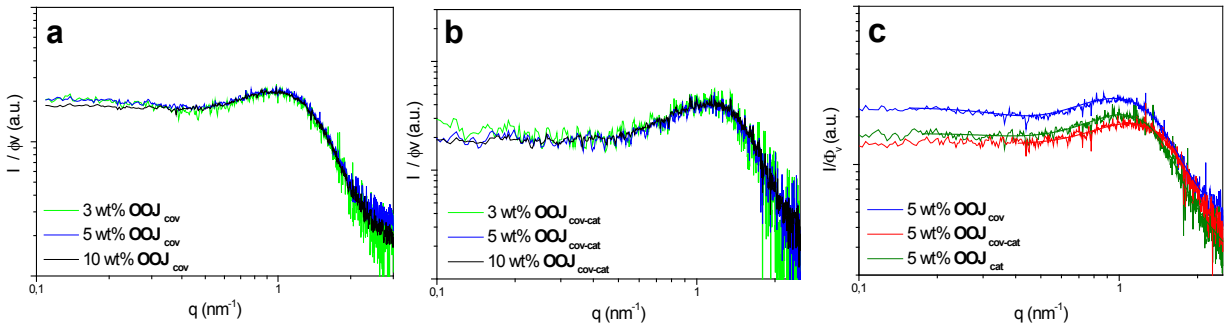

Figure S3. Experimental SAXS data (normalized with regard to the volume fraction of surfactant) of 3, 5, 10 wt% of $\mathbf{OOJ_{cov}}$ (a) and $\mathbf{OOJ_{cov\text{-}cat}}$ (b). Experimental and approximated (GIFT) SAXS data (normalized with regard to the volume fraction of surfactant) of $\mathbf{OOJ_{cov}}$, $\mathbf{OOJ_{cov\text{-}cat}}$ and $\mathbf{OOJ_{cat}}$ at a concentration of 5 wt% in water in log-log representation (c).

Calculation of the structural parameters:
For the *Im3m* cubic phase, the relation between the cell parameter ($a = 2\sqrt{d_{110}}$) and the hydrophobic radius R_H is determined from:

$$\frac{V_B}{V_S + \alpha V_W} = \frac{4\nu\,\pi R_H^{\,3}}{3a^3} \qquad (1)$$

where α stands for the number of water molecules per surfactant molecule, υ is the number of micelles per cubic lattice, (υ = 2 for Im3m phase), V_B, V_S, V_W respectively stand for the molar volumes of the hydrophobic part of the surfactant, the surfactant and water (V_W = 18 cm³/mol). V_B values were calculated by considering that the hydrophobic part consists in alkane chain and poly (oxypropylene), PPO units, whereas the hydrophilic part contains the polyoxyethylene, PEO units. These parameters have been calculated and the values are detailed in Table S4. The cross-sectional area S can then be deduced from the following relation, where N_A is the Avogadro's number:

$$S = \frac{3\,V_B}{N_A\,R_H} \qquad (2)$$

Similarly, the structural parameters of the hexagonal phase were determined from geometrical considerations. The Bragg distance d_{100} of the hexagonal phase can be related to the hydrophobic radius R_H by:

$$\frac{V_B}{V_S + \alpha V_W} = \frac{\pi\sqrt{3}R_H^{\,2}}{2d_{100}^2} \qquad (3)$$

The cross-sectional area S, considered as for cubic phase, at the polar-nonpolar interface lying between PEO and PPO, can be deduced in the same way from the following relation:

$$S = \frac{2\,V_B}{N_A\,R_H} \qquad (4)$$

Table S3. Variation of the structural parameters in function of α, the number of water molecules per surfactant molecule for **OOJ$_{cov\text{-}cat}$** and **OOJ$_{cat}$** in the *Im3m* phase

	alpha	a (nm)	R_H (nm)	S (nm²)
OOJ$_{cov\text{-}cat}$	131.9	8.98	2.88	1.86
	121.4	8.47	2.76	1.94
	111.8	8.35	2.77	1.94
OOJ$_{cat}$	120.3	7.84	2.56	2.14
	104.7	7.66	2.57	2.13
	71.0	7.19	2.57	2.13

Table S4. Molar volumes of the hydrophobic part of the surfactant, V_B and of the surfactant V_S for all studied systems. (considering d_{EO} =1.13 g/cm^3, d_{alkyl} = 0.9 g/cm^{3}and d_{PO} =1 g/cm^3)

	V_B (cm³/mol)	V_S (cm³/mol)
OOJ$_{cov}$	1055.6	1500
OOJ$_{cov\text{-}cat}$	1075.6	1518
OOJ$_{cat}$	1095.6	1536

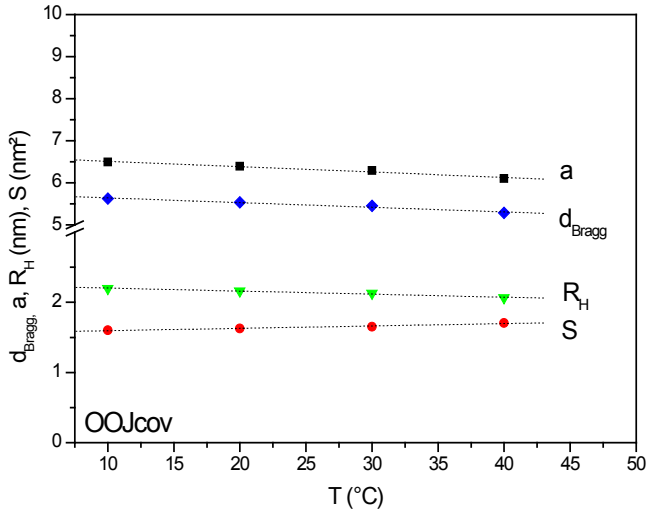

Figure S4. Variation of d spacing and structural parameters as a function of the temperature for **OOJ$_{cov}$** at 60 wt % in water.

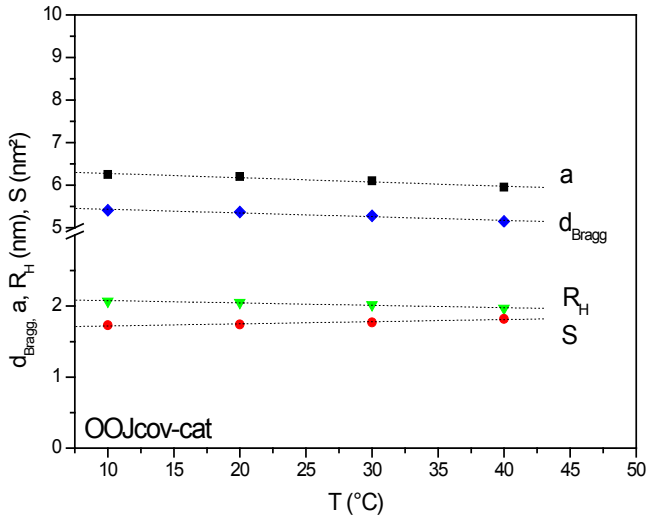

Figure S5. Variation of d spacing and structural parameters as a function of the temperature for **OOJ$_{cov\text{-}cat}$** at 56 wt % in water.

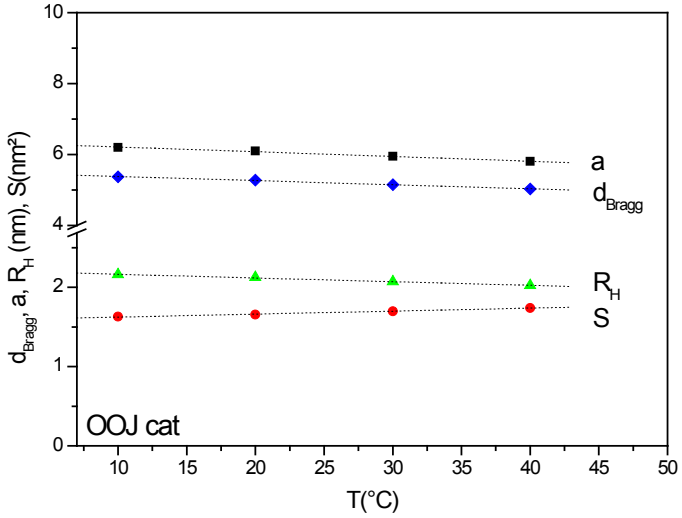

Figure S6. Variation of d spacing and structural parameters as a function of the temperature for **OOJ$_{cat}$** at 62 wt % in water.

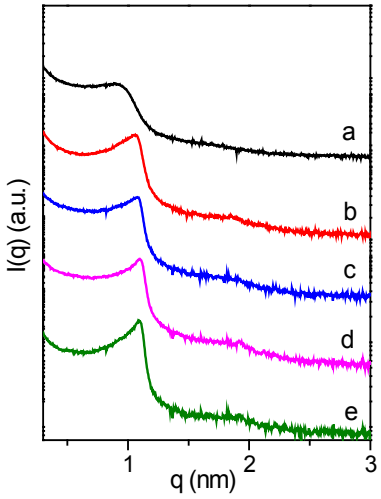

Figure S7. SAXS pattern evolution of the silica materials prepared with 5 wt% **OOJ$_{cov}$** at different molar ratio (surfactant/TMOS) R: (a) 0.9, (b) 0.4, (c) 0.2, (d) 0.125, (e) 0.075. All syntheses were performed during 48 h at 50 °C.

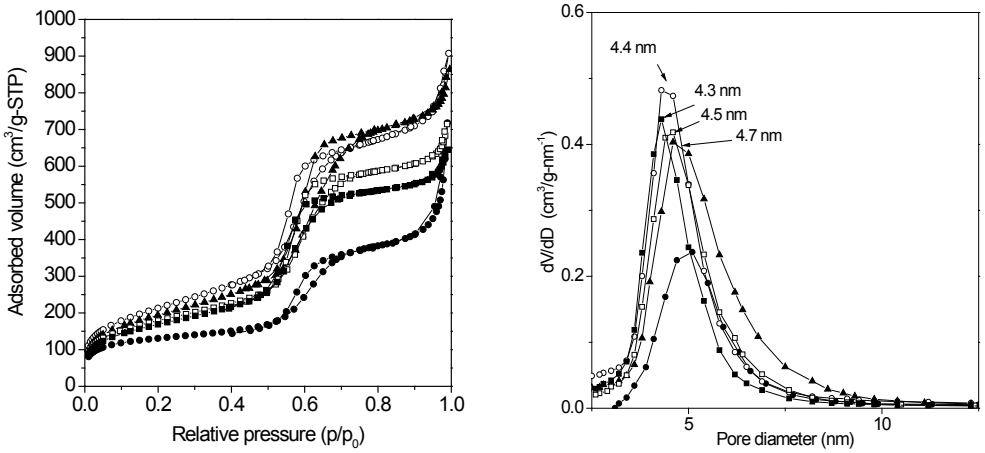

Figure S8. Nitrogen adsorption/desorption isotherms (left) and the pore diameter (right) of silica materials prepared from **OOJ$_{cov}$** at different molar ratio R: (●) 0.9, (○) 0.4, (▲) 0.2, (■) 0.125, (△) 0.075. All syntheses were performed during 48h at 50°C.

Table S5. Summary of the specific area (S_{BET}) and porous volume (V_p) values of the silica materials prepared during 48 h at 50 °C with 5 wt% **OOJ$_{cov}$** at different molar ratio (surfactant/TMOS) R

R	S_{BET} (m^2/g)	V_p (cm^3/g)
0.9	447	0.66
0.4	773	1.10
0.2	704	1.12
0.125	642	0.92
0.075	608	0.84

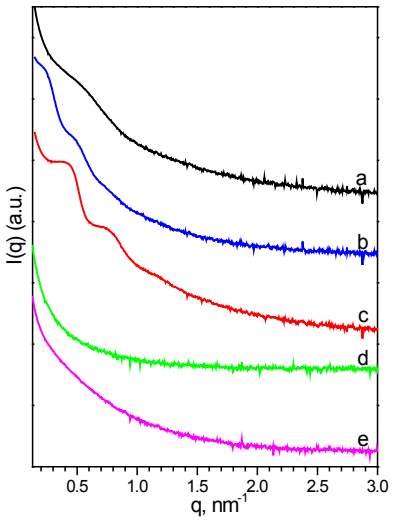

Figure S9. SAXS pattern evolution of the silica materials prepared with **OOJ$_{cat}$** in different reaction conditions of surfactant concentration, R ratio and hydrothermal synthesis temperature: (a) 5 wt%, R 0.05, RT, (b) 2.5 wt%, R 0.05, RT, (c) 1 wt%, R 0.05, RT, (d) 5 wt%, R 0.1, RT in comparison with (e) 5 wt%, R 0.1, 50°C.

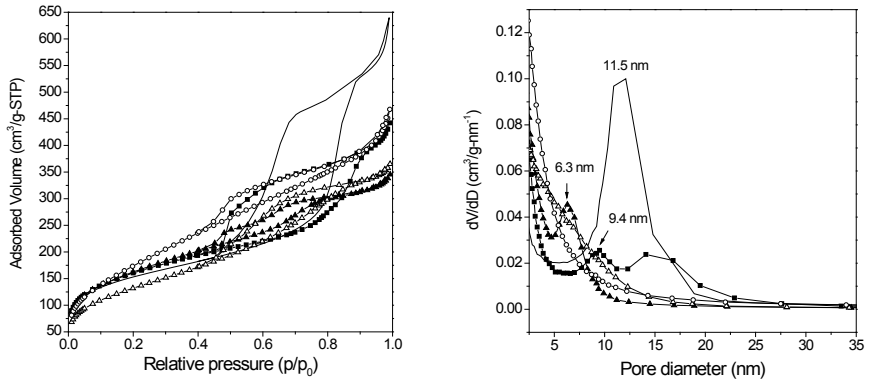

Figure S10. Nitrogen adsorption/desorption isotherms (left) and the pore diameter (right) of the silica materials prepared with **OOJ$_{cat}$** in different reaction conditions of surfactant concentration, R ratio and hydrothermal synthesis temperature: (▲) 5 wt%, R 0.05, RT, (■) 2.5 wt%, R 0.05, RT, (-) 1 wt%, R 0.05, RT, (○) 5 wt%, R 0.1, RT, (△) 5 wt%, R 0.1, 50°C.

Table S6. Summary of the specific area (S_{BET}) and porous volume (V_p) values for the **OOJ$_{cat}$**-based mesoporous silica materials.

Reaction conditions	S_{BET} (m^2/g)	V_p (cm^3/g)
5 wt% **OOJ$_{cat}$**, R 0.05, RT	659	0.52
2.5 wt% **OOJ$_{cat}$**, R 0.05, RT	483	0.45
1 wt% **OOJ$_{cat}$**, R 0.05, RT	536	0.76
5 wt% **OOJ$_{cat}$**, R 0.1, 50°C	570	0.50
5 wt% **OOJ$_{cat}$**, R 0.1, RT	583	0.38

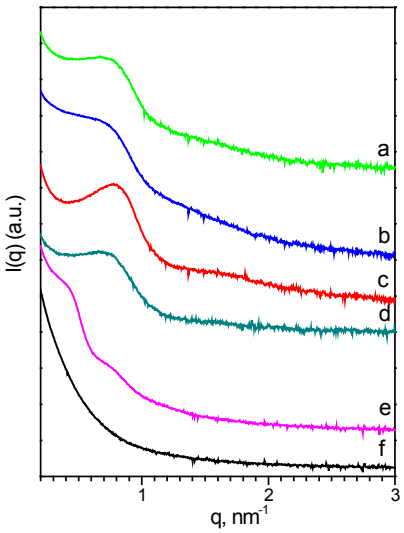

Figure S11. SAXS pattern evolution of the silica materials prepared from **OOJ$_{cov\text{-}cat}$** in different reaction conditions : (a) 5wt%, R 0.1, 40°C; (b) 5wt%, R 0.1, 50°C; (c) 5wt%, R 0.1, RT; (d) 5wt%, R 0.03, RT; (e) 1wt%, R 0.05, RT; (f) 1wt%, R 0.07, RT.

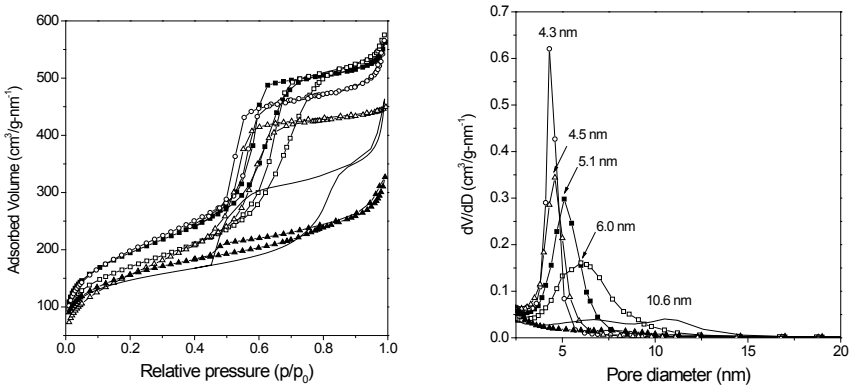

Figure S12. Nitrogen adsorption/desorption isotherms (left) and the pore diameter (right) of silica materials prepared from **OOJ$_{cov\text{-}cat}$** in different reaction conditions: (■) 5wt%, R 0.1, 40°C; (□) 5wt%, R 0.1, 50°C; (○) 5wt%, R 0.1, RT; (△) 5wt%, R 0.03, RT; (-) 1wt%, R 0.05, RT; (▲) 1wt%, R 0.03, RT.

Table S7. Summary of the specific area (S_{BET}) and porous volume (V_p) values for the **OOJ$_{cov\text{-}cat}$**-based mesoporous silica materials.

Reaction conditions	S_{BET} (m^2/g)	V_p (cm^3/g)
5 wt% **OOJ$_{cov\text{-}cat}$**, R 0.1, 40°C	692	0.72
5 wt% **OOJ$_{cov\text{-}cat}$**, R 0.1, 50°C	602	0.75
5 wt% **OOJ$_{cov\text{-}cat}$**, R 0.1, RT	717	0.67
5 wt% **OOJ$_{cov\text{-}cat}$**, R 0.03, RT	583	0.61
1 wt% **OOJ$_{cov\text{-}cat}$**, R 0.05, RT	506	0.47
1 wt% **OOJ$_{cov\text{-}cat}$**, R 0.07, RT	550	0.30